Pflügers Arch – Eur J Physiol (1996) 431 : 341–352

ORIGINAL ARTICLE

V. Magnelli · A. Avaltroni · E. Carbone

A single non-L-, non-N-type Ca^{2+} channel in rat insulin-secreting RINm5F cells

Received: 23 May 1995/Received after revision: 26 July 1995/Accepted: 15 August 1995

Abstract Single high-voltage-activated (HVA) Ca^{2+} channel activity was recorded in rat insulinoma RINm5F cells using cell-attached and outside-out configurations. Single-channel recordings revealed three distinct Ca^{2+} channel subtypes: one sensitive to dihydropyridines (DHPs)-(L-type), another sensitive to ω-conotoxin (CTx)-GVIA (N-type) and a third type insensitive to DHPs and ω-CTx-GVIA (non-L-, non-N-type). The L-type channel was recorded in most patches between -30 and +30 mV. The channel had pharmacological and biophysical features similar to the L-type channels described in other insulin-secreting cells (mean conductance 21 pS in control conditions and 24 pS in the presence of 5 μM Bay K 8644). The non-L-, non-N-type channel was recorded in cells chronically treated with ω-CTx-GVIA in the presence of nifedipine to avoid the contribution of N- and L-type channels. Channel activity was hardly detectable below -10 mV and was recruited by negative holding potentials (< -90 mV). The channel open probability increased steeply from -10 to + 40 mV. Different unitary current sublevels could be detected and the current voltage relationship was calculated from the higher amplitude level with a slope conductance of 21 pS. Channel activity lasted throughout depolarizations of 300–800 ms with little sign of inactivation. Above 0 mV the channel showed a persistent flickering kinetics with brief openings (τ_o 0.6 ms) and long bursts (τ_{burst} 60 ms) interrupted by short interburst intervals. The third HVA Ca^{2+} channel subtype, the N-type, had biophysical properties similar to the non-L-, non-N-type and was best identified in outside-out patches by its sensitivity to ω-CTx-GVIA. The channel was detectable only above -10 mV from a -90 mV holding potential, exhibited a fast flickering behaviour, persisted during prolonged depolarizations and had a slope conductance of about 19 pS. The present data provide direct evidence for a slowly inactivating non-L-, non-N-type channel in insulin-secreting RINm5F cells that activates at more positive voltages than the L-type channel and indicate the possibility of identifying unequivocally single HVA Ca^{2+} channels in cell-attached and excised membrane patches under controlled pharmacological conditions.

Key words Single Ca^{2+} channels · Dihydropyridines · ω-CTx-GVIA · Insulinoma · β-Cells

V. Magnelli · A. Avaltroni · E. Carbone (✉)
Dipartimento di Anatomia e Fisiologia Umana,
Corso Raffaello 30, I-10125 Turin, Italy

Introduction

Ca^{2+} entry through voltage-dependent Ca^{2+} channels is crucial for glucose-induced insulin release in pancreatic β-cells. Insulin secretion is regulated by the rhythmic behaviour of membrane potential, consisting of trains of fast Ca^{2+}-dependent spikes superimposed over slow potential oscillations (for a review see [2]). The role of voltage-dependent Ca^{2+} channels in this process is still controversial with regard to the channel subtypes involved [30]. To date, there is abundant evidence, at macroscopic and single-channel levels, for a low-threshold (LVA, T-type) Ca^{2+} channel [3, 28, 29] and a high-threshold channel (HVA, L-type) sensitive to dihydropyridines (DHPs) [27, 32, 35]. The latter contributes to most of the Ca^{2+} current and is ubiquitous in all insulin-secreting cells [2]. Recent reports, however, have provided increasing evidence for the existence, in β-cells and β-cell lines, of a significant DHP-resistant HVA current component [13, 25] that is partially blocked by ω-CTx-GVIA [31] and modulated by noradrenaline [25]. Electrophysiological [18] and molecular biology studies [15] have also provided evidence for the existence in rat islets and RINm5F cells of a class A Ca^{2+} channel (Q-, or P-type) that is resistant to DHP, ω-CTx-GVIA and high doses of ω-agatoxin-IVA (ω-Aga-IVA), but is sensitive to micromolar

concentrations of ω-CTx-MVIIC. The channel contributes to approximately 35% of the total HVA current in RINm5F cells and is responsible for most of the non-L-type component. To date, however, there are no available data of single-channel currents supporting the presence of a DHP- and ω-CTx-GVIA-resistant channel in insulin-secreting cells. This may be due to its low density of expression in rodent and human β-cells and to technical difficulties in recording single Ca^{2+} channel activity.

Based primarily on pharmacological grounds, here we present evidence for a single DHP- and ω-CTx-GVIA-resistant channel that coexists with the common L-type channel in cell-attached and outside-out patches of RINm5F cells. The non-L-, non-N-type channel activates at potentials more positive than the L-type, inactivates slowly during long depolarizations and possesses a single-channel conductance comparable to that of other HVA Ca^{2+} channels (18–20 pS). Its inactivation kinetics and holding potential sensitivity are close to those of the slowly inactivating G1-type channel of rat cerebellar granule cells [10] and the α_1 isoform of the rat brain class A channel, rbA-II, expressed in oocytes [33], but differ partially from those of the P-type channel of cerebellar Purkinje neurons [34] and the fast inactivating Q-type channel of cerebellar granule cells [26]. The non-L-, non-N-type channel reported here, accounts nicely for the sustained "Q-like" current identified in RINm5F cells [18] and may be related to the slowly inactivating DHP-resistant Ca^{2+} current observed in rodent pancreatic β-cells which is proposed to underlie burst duration during β-cell electrical activity [13, 30].

A preliminary account of this work has already appeared in abstract form [17].

Materials and methods

Cell culture

The rat insulinoma cell line RINm5F was kindly provided by Dr. C.B. Wollheim (Centre Médical Universitaire, Geneva, Switzerland). Cells, maintained in 10-mm plastic Petri dishes, were grown in RPMI-1640 medium (Sigma, St. Louis, Mo, USA) supplemented with 10% heat-inactivated fetal calf serum, 100 IU/ml penicillin and 100 µg/ml streptomycin, 2 mM l-glutamine. Cells were grown to confluency, split every 7 days by trypsin treatment and incubated in 5% CO_2 at 37° C. Experiments were performed 3–7 days after plating.

Solutions

In cell-attached patch experiments the external bathing solution contained (mM): 135 potassium aspartate, 1 $MgCl_2$, 10 4-(2-hydroxyethyl)-1-piperazineethanesulphonic acid (HEPES, pH 7.3 with KOH) and 5 ethylenebis(oxonitrilo)tetraacetate (EGTA) to zero the resting membrane potential. To increase the signal-to-noise ratio of single Ba^{2+} current recordings, the pipette filling solution contained (in mM): 100 $BaCl_2$, 10 tetraethylammonium chloride (TEACl), 1 $MgCl_2$ and 10 HEPES (pH 7.3 with TEAOH). Tetrodotoxin (TTX) was added at 300 nM concentration to block Na^+ channels. In outside-out patch experiments the external bath contained (in mM): 100 $BaCl_2$, 10 TEACl, 1 $MgCl_2$ and 10 HEPES (pH 7.3 with NaOH) with 300 nM TTX. The electrode filling solution was (in mM): 110 CsCl, 30 TEACl, 10 EGTA, 1 $MgCl_2$, 10 HEPES (pH 7.3 with CsOH), 2 adenosine 5′-triphospate (ATP) and 0.25 adenosine 3′-5′-cyclic monophospate (cAMP). Bay K 8644 and nifedipine were from Bayer (Wuppertal, Germany) and prepared as 1 mM stock solutions in 100% ethanol and stored light-protected at 4° C. Both drugs were used at 5 µM final concentration and applied in 100 mM Ba^{2+} to either whole-cell, cell-attached or outside-out patches, with the same potency. Due to membrane diffusion limitations, however, the action of the DHPs applied to the exterior of the recording pipette required 1–2 min to achieve maximal efficacy in the cell-attached configuration. In contrast, the effects of the DHPs were very fast in outside-out patches. ω-CTx-GVIA (Bachem, Bubendorf, Switzerland) was dissolved in distilled water and frozen at −20° C. To maximize its blocking action, the toxin was dissolved in a standard Tyrode solution (mM): 150 NaCl, 4 KCl, 2 $MgCl_2$, 2 $CaCl_2$, 10 glucose and 10 HEPES and applied for 1–2 min to block irreversibly the N-type channel [31].

The perfusion system consisted of a multi-barrelled glass pipette held close to the sealed cell or excised patch in which four stainless steel needles were allocated. Perfusion solutions were passed through Teflon syringes and tubes to avoid non-specific binding to plastic materials. When acutely applied to the cell, ω-CTx-GVIA was delivered through a separate glass pipette kept out of the bath and moved close to the cell immediately before toxin application. Due to the slow washing out of the toxin in 100 mM Ba^{2+} solutions [12, 31], the dish was changed after each cell recording.

Patch electrodes and data acquisition

Patch electrodes were pulled from thick-walled borosilicate glasses (Hilgenberg, Malsfeld, Germany) on a two-step vertical puller (Narishige Scientific, Tokyo, Japan). To reduce the electrode capacitance, the tapered region of the pipettes was coated with Sylgard 184 (Dow Corning, Midland, Mich, USA) down to 10 µm from the tip and cured in a heated coil under an inverted microscope at low magnification (x 100). The coated electrodes were then fire polished immediately before use on a Narishige vertical microforge. The final pipette resistance ranged typically between 7 and 9 MΩ for cell-attached recordings and between 5 and 7 MΩ for outside-out patches. The reference electrode was a silver-silver chloride pellet connected to the bath through an agar bridge (1 M KCl). Junction potential with the solutions employed was between 3 and 4 mV and not corrected since the ionic content of the pipette and bath solutions remained unchanged in most of our experiments.

The plastic Petri dishes containing the cells were mounted on a Wilovert S inverted phase-contrast microscope (Hund, Wetzlar, Germany) at high magnification (x 400). Single-channel activity was recorded in cell-attached and outside-out configurations according to the method already described [11]. Currents were recorded with a List EPC-7 amplifier (List Electronic, Darmstadt, Germany) through a 50 GΩ feedback resistor, filtered at 2 kHz with an 8-pole low-pass Bessel filter and acquired at intervals of 100–200 µs per point. Membrane stimulation and data acquisition were performed by using pClamp software (Axon Instrument, Foster City, Calif, USA) and a 12-bit A/D Tecmar Lab Master board (125 kHz) interfaced with an IBM-compatible personal computer. Voltage pulses of 100–300 ms duration and variable amplitude were delivered at intervals of 5–10 s both to limit the rundown of Ca^{2+} channels and to allow their recovery from inactivation. The holding potential varied from −40 to −100 mV as required.

Capacitative transients were minimized on-line by patch-clamp analogue compensation. The residual capacitative and leak currents were corrected off-line during the analysis by subtracting either an average of "null" sweeps, or the current traces recorded during

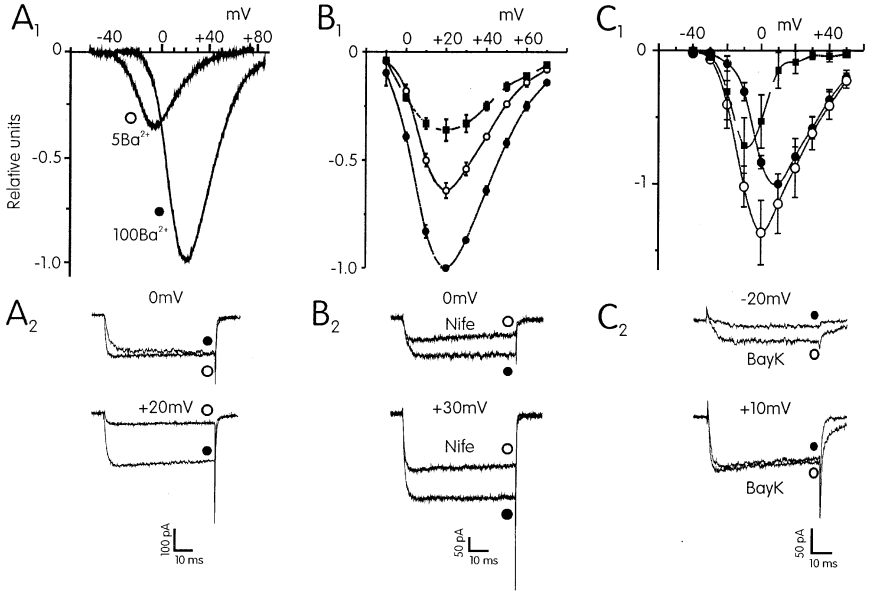

Fig. 1A–C Whole-cell Ba^{2+} currents in low and high $[Ba^{2+}]_o$: effects of dihydropyridines (DHPs). A I/V curves and time course of Ba^{2+} currents in 5 mM (○) and 100 mM (●) Ba^{2+}. The I/V traces are average currents recorded from 5 cells during a depolarizing ramp of 2 mV/ms from −90 mV holding potential, V_h (**A_1**). Increasing external $[Ba^{2+}]_o$ resulted in a + 28 mV shift of the peak current due to the screening of membrane surface charges by Ba^{2+} ions. **A_2** Time course of Ba^{2+} currents in 5 (○) and 100 mM Ba^{2+} (●) at the potential indicated. **B, C** In 100 mM Ba^{2+} the high-voltage-activated (HVA) current is sensitive to DHPs in cells chronically treated with ω-CTx-GVIA. Nifedipine (5 μM) reduces the control inward current (● in **B_1**) at test potentials of −10 to + 70 mV in a voltage-dependent manner (○) (mean ± S.E.M., n = 6 cells). The I/V relationship of the DHP-sensitive component is indicated by the *dashed line* through ■ (**B_1**). Representative currents at 0 mV and + 30 mV are shown in **B_2** before (●) and after (○) application of nifedipine (nife) ■. The agonist Bay K 8644 (5 μM) increases the control HVA currents between −40 and + 10 mV (○ in **C_1**) shifting the peak of the I/V curve by −15 mV (○) (mean ± SEM, n = 6 cells). The I/V curve of Bay K 8644-modified currents is indicated by the *dashed line* and ■. The agonistic effects of Bay K 8644 are visible from the Ba^{2+} current increase at −20 mV and the slow down of tail currents upon repolarization to −35 mV (**C_2**).

application of 200 μM $CdCl_2$ to outside-out patches. Subtraction of Cd^{2+}-insensitive currents was essential when single-channel activity was high and probability of recording blank sweeps was low. All the experiments were performed at room temperature (20–22° C).

Data analysis

Unitary events were analysed as described previously [4] using AutesP software (Garching Innovation, Munich, Germany). Channel openings were detected by the half-amplitude criterion [7] and converted into idealized events by means of interactive fitting routines [4]. Open and closed durations were measured on idealized records by setting the minimum resolvable time to 200–300 μs. Fits of amplitude histograms, open and closed time distributions were performed with the maximum-likelihood algorithms. For each sweep and for patches containing only one channel the open probability (p_o) was calculated as: $p_o = t_o/(t_o + t_c)$ where t_o and t_c represent the total time the channel spent in the open and closed state, respectively. Activation curves, $p_o(V)$, were obtained by averaging the p_o values at a given voltage over a number of sweeps.

The channel conductance and the corresponding single-channel current voltage relationship (i/V) were estimated by measuring the unitary current amplitude at potentials ranging between −30 and + 30 mV. At greater depolarizations, the channel amplitude was too small (< 0.2 pA) to be resolved from the background noise, while at lower depolarizations the probability of opening was too low to obtain a sufficient number of well-resolved unitary events. Ensemble currents were obtained by averaging a variable number of sweeps previously corrected for the capacitative artifact as described above. All data are given as mean ± SEM for n number of observations. Statistical significance (P) was calculated using the Student's t-test.

Results

Whole-cell currents in 100 mM Ba^{2+}

Single channel recordings are usually determined in extracellular solutions containing high $[Ba^{2+}]$ (50–100 mM) while whole-cell currents are recorded in low $[Ba^{2+}]_o$ solutions (2–10 mM). Normally, increasing $[Ba^{2+}]_o$ from 5 to 100 mM causes a 25 to 30 mV positive shift in the voltage-dependent parameters of Ca^{2+} channels [9]. However, in some case, high $[Ba^{2+}]_o$ also reveals Ba^{2+} currents that are not evident at lower $[Ba^{2+}]_o$ and could be erroneously attributed to other Ca^{2+} channels during unitary current recordings [8]. To assay for the existence of any "latent" Ba^{2+} current and to determine the exact voltage range of activation of the various single Ca^{2+} channels in high $[Ba^{2+}]_o$, we first studied the voltage-dependent features of whole-cell currents in 100 mM Ba^{2+}. As shown in Fig. 1A, increasing $[Ba^{2+}]_o$ from 5 to 100 mM shifted the activation range of HVA currents by 28 mV to more positive potentials and caused no changes to the overall shape of the I/V relationships. Despite the threefold-

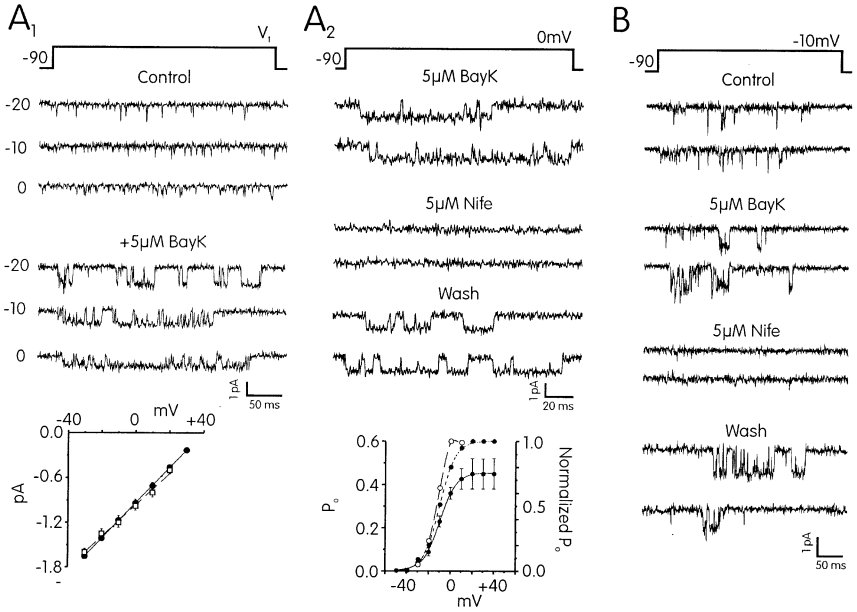

Fig. 2A, B DHP-sensitive channels in cell-attached (**A**) and outside-out (**B**) patches of RINm5F cells. **A_1** Unitary L-type currents in control conditions and in the presence of 5 μM Bay K 8644 at −20, −10 and 0 mV test potentials from −90 mV V_h. The membrane resting potential is zeroed by perfusing the sealed cell with 135 mM potassium aspartate. Single-channel openings are notably prolonged after adding Bay K 8644 to the bath. The *bottom panel* shows unitary i/V relationships for the DHP-sensitive channel in control conditions (□) and after addition of Bay K 8644 (●). Data points were collected from 8 patches in both cases. The linear fit of control data (*dashed line*) gave a slope conductance, γ, of 21.1 pS while for Bay K 8644-modified channels, γ was 23.7 ± 0.9 pS n = 12 (*solid line*). **A_2** In cell-attached patches, the L-type channel is sensitive to external application of DHP agonists and antagonists. Bay K 8644 prolongs the channel mean open time (*top traces*) while nifedipine completely abolishes the channel activity within 2 min (*middle traces*). Replacement of nifedipine with Bay K 8644 restores in 3 min the previous activity (*bottom traces*). Probability of single L-type channel opening and macroscopic Ba^{2+} conductance (g_{Ba}) versus voltage are compared in the *bottom panel*. The data represent averages of absolute (● and *solid line*) and normalized values (● and *dotted line*). Data points are fitted by a Boltzmann function, $p_o = p_{omax}\ (1 + exp\ [(V_{½}\text{-}V)/k])^{-1}$ with $V_{½} = -10.4$, $k = 7$ mV and $p_{omax} = 0.43$ and 1, respectively. The *empty circles* and *dotted line* are normalized values of g_{Ba} derived from the I/V curve of Bay K 8644-modified currents (○ in Fig. 1C) and calculated from $g_{Ba} = I_{Ba}/(E\text{-}E_{Ba})$, with the Ba^{2+} equilibrium potential, $E_{Ba} = +70$ mV. **B** DHP-sensitive channel activity recorded from an outside-out patch bathed in 100 mM Ba^{2+} in control conditions (*two top traces*), during exposure to Bay K 8644 (*third and fourth trace from top*), nifedipine (*fifth and sixth trace from top*) and Bay K 8644 again (*two bottom traces*). Test potential and holding potential as indicated

increase of the maximal current, there was no sign of Ba^{2+} currents activation at low voltages; neither in the early part of the I/V curve determined by ramp commands (Fig. $1A_1$) nor in the current recordings during step depolarizations above −30 mV (Fig. $1A_2$). The kinetics of HVA channel activation in high $[Ba^{2+}]_o$ underwent the same voltage shift of the I/V characteristics (not shown). At 0 mV, the current in 100 mM Ba^{2+} raised more slowly than that in 5 mM Ba^{2+} (time constant of activation, τ_{act} 2.4 ms vs 0.8 ms; Fig. $1A_2$ top) while at + 20 mV the two currents activated equally fast (τ_{act} 1.1 vs 0.8 ms; Fig. $1A_2$ bottom). Time-dependent inactivation was slow and largely incomplete in low and high $[Ba^{2+}]_o$ solutions during pulses of 60 to 100 ms. Inactivation was not evident even at + 20 mV, despite the current in 100 mM Ba^{2+} (●, bottom) was fourfold larger than that in 5 mM Ba^{2+} (○, bottom).

The voltage dependency of non-L, non-N-type currents in high $[Ba^{2+}]_o$ solutions was determined in ω-CTx-GVIA-treated cells deprived of N-type channels (Fig. 1B). As in low $[Ba^{2+}]_o$ solution [18], 5 μM nifedipine caused a marked depression of HVA currents below 0 mV with respect to more positive voltages: 57% and 38% block after 100 ms at 0 and + 30 mV (Fig. $1B_2$ and, ○ in Fig. $1B_1$). The I/V curves resulting from the subtraction of control and nifedipine-resistant currents (*nifedipine-sensitive*; ■ and dashed line) revealed that, as in low $[Ba^{2+}]_o$ [25], the L-type current activates at slightly more negative potentials with respect to the non-L-, non-N-type current (○ and solid line). Half-maximal activation ($V_{½}$) of the L-type current was around −2 mV compared to the + 6 mV of the non-L-, non-N-type component. There was, however, some variability between the two $V_{½}$ values depending on the cell type. The $V_{½}$ differed by 7–12 mV, which corresponded reasonably well with the voltage separation estimated in low $[Ba^{2+}]_o$.

Since we used Ca^{2+} channel agonists to reveal single L-type channels [32], we also determined the voltage dependency of L-type currents in the presence of Bay K 8644 in high $[Ba^{2+}]_o$ solution (Fig. $1C_1$). As for low $[Ba^{2+}]_o$, saturating doses of the agonist (5 μM) caused a marked increase of L-type currents at

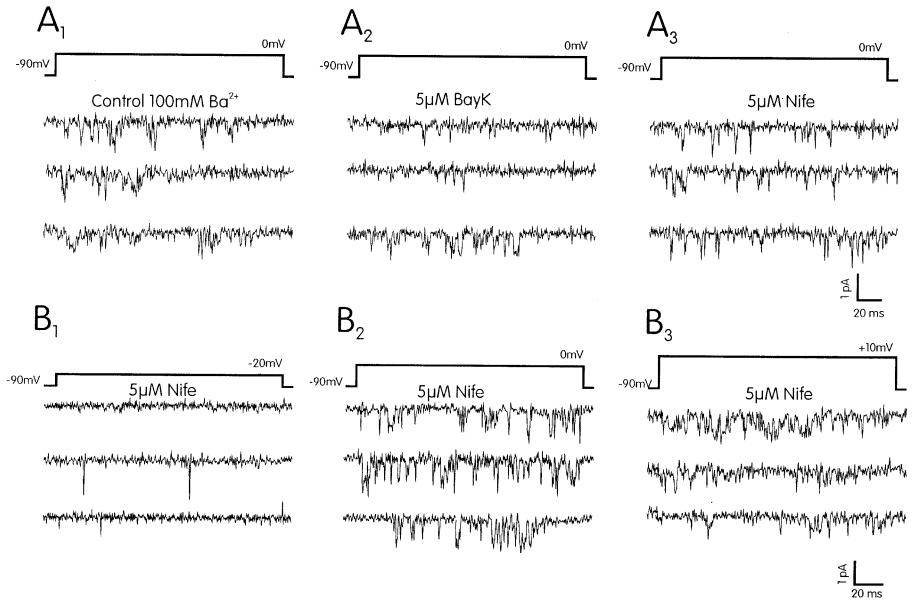

Fig. 3A, B DHP-resistant channels in cell-attached patches of RINm5F cells. **A** Selected traces of single non-L-type channel activity evoked with 200 ms step depolarizations to 0 mV from −90 mV V_h. Channel openings in control conditions (**A_1**) are unaffected by Bay K 8644 (**A_2**) and persist in the presence of nifedipine (**A_3**). **B** Non-L-type channel activity recorded in the presence of 5 μM nifedipine at different voltages. Notice the presence of null sweeps and the few brief openings at −20 mV (**B_1**). Probability of channel openings increases sharply at 0 mV (**B_2**) and + 10 mV (**B_3**). V_h −90 mV

−20 mV and little change at + 10 mV. At this potential the L-type channel contributes relatively less to the total current. The I/V relationships in the presence of Bay K 8644 were shifted by −15 mV, with a corresponding increase of Ba^{2+} currents at potentials below 0 mV. The $V_{½}$ value for the Bay K 8644-modified currents was −19 mV (dashed line and ■ in Fig. 1C_1).

Single L-type channels in cell-attached and outside-out patches

Single L-type channels in 100 mM Ba^{2+} could be detected in 79% of cell-attached patches in a total of 154 RINm5F cells. Brief openings of the channel were already evident during 300 ms-long depolarizations to −20 mV. The p_o was 0.024 (n = 20) at −20 mV and increased to 0.095 at 0 mV (n = 12) (Fig. 2A_1). The channel had a mean unitary current of −1.15 pA at -10 mV and 21.1 ± 2.4 pS (n = 8) slope conductance (γ), (○ in Fig. 2A_1 bottom). The identity of L-type channels was ensured by either testing the agonistic action of Bay K 8644, or the blocking effects of nifedipine externally applied to the cell (Fig. 2A_2). Both DHPs required 1–2 min to reach maximal effects and 2–3 min to be washed out. Application of 5 μM Bay K 8644 caused well-resolved long-lasting openings, with about tenfold larger mean open times (τ_o 0.35 ms in control conditions and 4.5 ms in the presence of Bay K 8644). p_o also increased from 0.024 to 0.102 at −20 mV with the agonist to reach maximum values of 0.45 above + 10 mV (Fig. 2A_2 bottom). The mean γ of Bay K 8644-modified channels was 23.7 ± 0.9 pS (n = 12) (● in Fig. 2A_1 bottom).

L-Type channel activity could be recorded also in outside-out patches provided that the pipette contained 0.25 mM cAMP and 4 mM MgATP to reduce channel run down (Fig. 2B). There was, however, larger variability in the percentage of successful patches with sustained Ca^{2+} channel activity compared to the cell-attached conditions. Very likely, the stability of outside-out patches depended upon some uncontrolled factor related either to the cell condition, the size of the excised membrane and the amount of protoplasm sucked into the pipette while forming the patch. The elementary properties of the L-type channel were apparently unaffected by membrane excision. Brief and repeated openings were already evident at and below −10 mV. Application of Bay K 8644 or nifedipine caused either prolongation or full block of channel activity (mean γ 24 pS, Fig. 2B). The action of both drugs was fast (onset 1–2 s), while their wash out required 40–60 s. This was true also for Cd^{2+} (200 μM) that quickly and reversibly blocked single L-type channels (not shown).

Non-L-type channels in cell-attached patches

Out of 154 cell-attached patches held at −90 mV holding potential, 45 were found to possess DHP-insensitive Ca^{2+} channels whose activity persisted in the presence of 5 μM nifedipine and showed no obvious prolongation with 5 μM Bay K 8644 (Fig. 3A). The activity of DHP-resistant channels (non-L-type) was steeply voltage dependent and required very negative holding potentials to be recruited (−90 mV). Unlike L-type channels, non-L-type channel activity decreased markedly at holding potentials beyond −60 mV. With 5 μM nifedipine inside and outside the pipette, repeated openings of non-L-type channels were apparent only above 0 mV (Fig. 3B). At −20 mV, the channels opened rarely and briefly during pulses of 150–300 ms

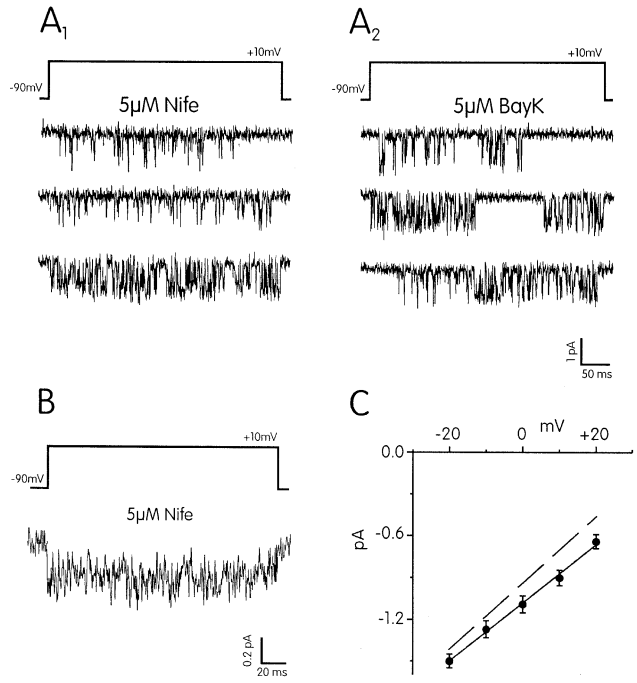

Fig. 4A–C Single non-L-, non-N-type channel in cell-attached patches of ω-CTx-GVIA-treated RINm5F cells. **A** Representative current traces recorded at + 10 mV from a RINm5F cell chronically pre-treated with 6.4 μM ω-CTx-GVIA (20 min in 2 mM $[Ca^{2+}]_o$ solution). The step depolarizations lasted 500 ms and were evoked every 10 s from −90 mV V_h. Non-L, non-N-type channel activity persisted in the presence of nifedipine (**A_1**) and showed no visible prolongation in the presence of Bay K 8644 (**A_2**). **B** Ensemble non-L-, non-N-type currents obtained by averaging 30 single channel traces at + 10 mV under the same conditions of panel **A_1**. **C** Unitary i/V relationships for the non-L-, non-N-type channel of a ω-CTx-GVIA-treated patch plus nifedipine. The regression line through the data points has a slope of 20.9 ± 2.3 pS (n = 5). The *dashed line* represents the i/V relationship of the Bay K 8644-modified L-type channel derived from data in Fig. **$2A_1$**. Notice the different slope and slight voltage shift between the two lines

duration while at 0 mV they exhibited higher p_o values, persistent bursts of activity and little sign of time-dependent inactivation during prolonged depolarizations.

Despite non-L-type currents in nifedipine-treated RINm5F cells were expected to be carried by two distinct non-L-type channels (N-type and Q-like; [18]), single-channel recordings showed no significant differences whether obtained from control cells (n = 91) containing both channels or from cells chronically treated with ω-CTx-GVIA (n = 63) containing only Q-like channels. The p_o value, γ and the inactivation time course were not significantly different in the two groups of cells, suggesting that either detection of N-type channels was unlikely or that the two channels possessed similar biophysical properties. The issue of separating N-type from Q-like channels in cell-attached patches was further complicated by the limitations of the recording conditions. There was no way to block either one of the two channels by acutely applying selective toxins outside the recording pipette. The possibility of isolating N-type from P- or Q-like channels by chronic treatment with 10 μM ω-CTx-MVIIC (30 min, [12]) was biased by the partial leaky conditions of the cells after toxin treatment. For these reasons the separation of the two non-L-type channels was postponed to more suitable patch configurations (see below) and the attention focused on the properties of non-L, non-N-type channels in cell-attached patches of RINm5F cells chronically treated with ω-CTx-GVIA.

Non-L-, non-N-type channels in cell-attached patches

Figure 4 shows unitary currents recorded at +10 mV from a cell incubated for 20 min in low $[Ca^{2+}]_o$ solutions containing 6.4 μM ω-CTx-GVIA, i.e. deprived of N-type channels. The absence of L-type channels was ensured by the persistent channel activity in the presence of 5 μM nifedipine (Fig. $4A_1$) and lack of agonistic effects with Bay K 8644 (Fig. $4A_2$). Given the low rate of toxin unbinding in high $[Ba^{2+}]_o$ solutions and the low density of N-type channels in RINm5F cells, the recordings of Fig. 4 were likely from a non-L, non-N-type channel. Several lines of evidence support this view. Similar to the Q-like current recorded in the presence of 100 mM Ba^{2+} (Fig. 1B), the channel activated positive to −10 mV (Fig. 5A) with steep voltage dependency. The p_o was around 0.03 at −10 mV, increased to 0.20 at + 10 mV and reached maximal values of 0.38 above + 30 mV (● in Fig. 5B). The $V_{½}$ value was at + 7.9 mV, which is very close to the $V_{½}$ of the normalized Ba^{2+} conductance (g_{Ba}) calculated for the Q-like current in 100 mM Ba^{2+} ($V_{½}$ + 6 mV; ○ in Fig. 5B). Like other HVA channels, the amplitude of unitary events was resolved by a broad Gaussian distribution at + 10 mV that resulted from either partially unresolved brief openings of smaller amplitude or subconductance levels of the same channel (Fig. 5C). Similar to the single P-type channel in cerebellar granules [34] we could distinguish two or even three sublevels of channel conductance, but we found no rigorous criteria to justify them. We therefore focused on the i/V relationship of the higher conductance level that represented, in all cases, the most frequently occupied one at all potentials (γ 20.9 ± 2.3 pS, n = 5; ● in Fig. 4C). Compared to that of Bay K 8644-modified L-type channels (dashed line in Fig. 4C), the i/V relationship of the non-L-, non-N-type channel was found to be less steep, slightly shifted and statistically well separated ($P < 0.005$). Statistical significance, however, was very poor when comparing the γ of the Q-like channel with that of the normal L-type channel (γ 21.1 ± 2.4 pS, n = 8, $P < 0.8$).

Activation of the channel was fast and inactivation was nearly undetectable in ensemble currents at + 10 mV during pulses of 200 ms duration (Fig. 4B). In some patches and at a given potential, the channel

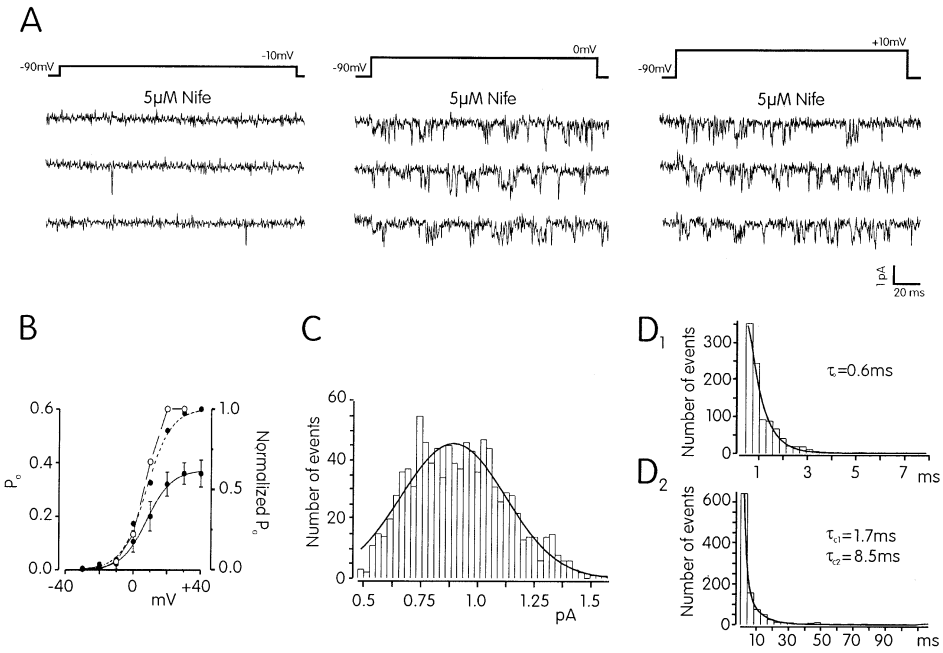

Fig. 5A–D Kinetics and voltage-dependent activation of the non-L-, non-N-type channels in ω-CTx-GVIA-treated RINm5F cells. **A** Three representative traces of the non-L-, non-N-type channel activity recorded at −10, 0 and + 10 mV in a cell-attached patch formed from a ω-CTx-GVIA-treated cell. The recordings are obtained in the presence of nifedipine to ensure the block of L-type channels. Notice the low probability of openings at −10 mV, which increases steeply at higher voltages. V_h −90 mV. In **B,** the absolute (● and *solid line*) and normalized (● and *dotted line*) values of p_o as a function of voltage are reported; data are derived from 3 cells treated as described in panel *A*. The *empty circles* represent the g_{Ba} derived from the I/V curve of the nifedipine-resistant currents in Fig. 1B (○) and calculated as in Fig. 2B with E_{Ba} = + 90 mV. **C** Amplitude histogram of non-L, non-N-type channels at 0 mV. Data points were obtained from 3 cells and fitted with a Gaussian distribution with a mean of -0.87 pA and standard deviation 0.22 pA. **D** Open and closed time distributions at 0 mV. The distributions were fitted with exponential functions by best fitting routines described elsewhere [4]. Estimated mean open and closed times were: τ_o 0.6 ms (**D_1**) and τ_{c1} 1.7 ms and τ_{c2} 8.5 ms (**D_2**)

showed periods of reduced activity followed by periods of high activity in which channel activity was burst-like for the entire pulse length (first and third trace in Fig. $4A_1$). Channel bursting was often followed by prolonged closures (second trace in Fig. $4A_2$) that complicated the analysis of channel opening and closing. Channel openings within a burst were fast (τ_o 0.6 ms) and followed by short closures (τ_{c1} 1.7 ms) (Fig. $5D_1$,D_2). Bursts lasted 60 ms, on average, and were separated by average interburst intervals of 8.5 ms (τ_{c2}).

N-type and Q-like channels in outside-out patches

Outside-out patches overcame some of the technical shortcomings of cell-attached recordings and allowed to identify single N-type channels in RINm5F cells. To discriminate between N-type and Q-like channels, single DHP-insensitive channels were tested for their sensitivity to ω-CTx-GVIA (6.4 μM), applied for 1 min in normal Tyrode solution. These conditions were found to be sufficient to ensure full block of N-type channels in a time interval shorter than the life-time of channel run down in excised patches (5–10 min). Non-L-type channels persisting after toxin application were classified as Q-like; those irreversibly blocked by the toxin as N-type. Figure 6A shows recordings of the N-type channel at + 10 mV in an outside-out patch formed with 5 μM nifedipine inside and outside the patch pipette. Under similar conditions, single and multiple N-type channels were detected in 3 out of 11 outside-out patches tested for the action of ω-CTx-GVIA. The activity of the N-type channel was similar to that of the Q-like channel. The N-type channel was active above −10 mV and had a steeply voltage-dependent p_o value. The channel also showed fast activation and persistent bursts of activity during pulses of 250 ms (Fig. $6A_1$), resulting in ensemble currents of slow and incomplete inactivation (Fig. 6C). The mean slope conductance of the channel was 19 ± 2.1 pS (Fig. 6B) and, thus, not significantly different from the 20.9 ± 2.3 pS of the non-L-, non-N-type channel ($P < 0.2$) . At + 10 mV τ_o was 1.1 ms (Fig. $6D_1$); τ_{c1} and τ_{c2} were 1.3 and 10.1 ms respectively (Fig. $6D_2$). Comparable values were found for the Q-like channel at the same voltage (τ_o 0.9 ms and τ_{c1} 2.0 ms). Given these similarities, the possibility that disappearance of Ca^{2+} channel activity during ω-CTx-GVIA application could derive from a quick run down of Q-like channels cannot be ruled out. Contrary to this, however, a genuine block of N-type channels by ω-CTx-GVIA is supported by the following observation: (1) toxin application was

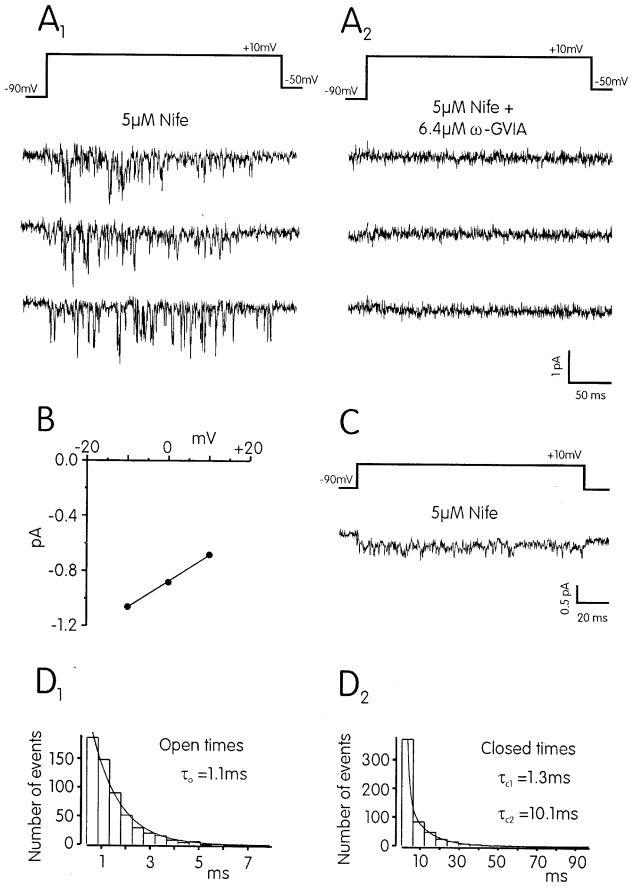

Fig. 6A–D Pharmacological identification of N-type channels in outside-out patches. **A** Unitary currents recorded in 100 mM Ba^{2+} before (A_1) and after (A_2) acute application of 6.4 μM ω-CTx-GVIA (1 min in 2 mM Ca^{2+}) to an outside-out patch. The bath solution contained 5 μM nifedipine to ensure the block of L-type channels. Test depolarizations were to + 10 mV from V_h −90 mV. Notice the total absence of channel activity and leakage current after toxin application. **B** Unitary i/V relationship of the N-type channel derived from one patch. The regression line through data points has a slope of 19 pS. **C** Ensemble N-type currents obtained by averaging 28 traces from 3 patches treated as described in **A**. **D** Open and closed time distributions at + 10 mV obtained from 3 outside-out patches. Mean open and closed times are as indicated

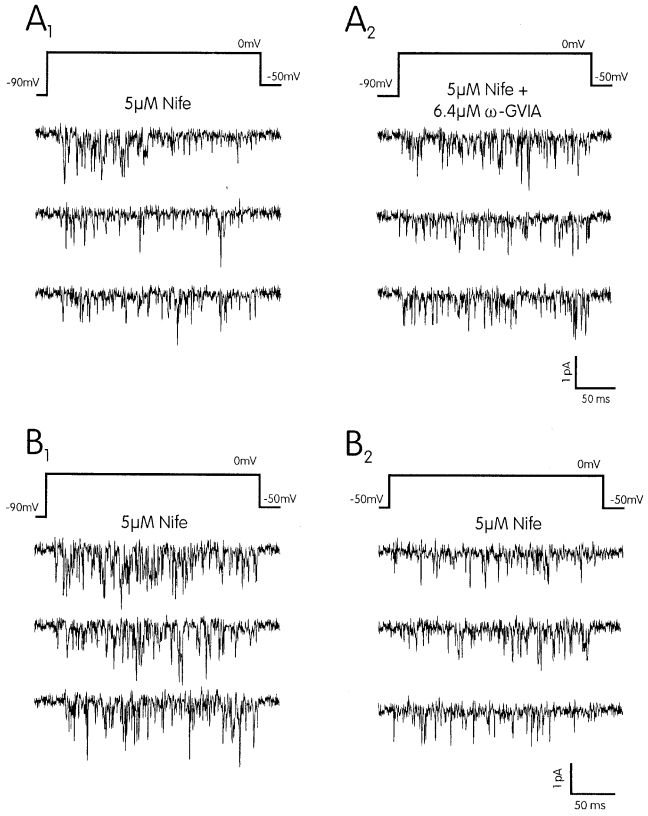

Fig. 7A–B Non-L-, non-N-type channels in outside-out patches: kinetics and sensitivity to V_h. **A** Representative traces of DHP-resistant channels that persist after application of ω-CTx-GVIA to an outside-out patch of a RINm5F cell. Notice the sustained channel activity after the toxin application and the presence of nifedipine. Same pharmacological conditions as described in Fig. 6A. Test depolarizations to 0 mV from −90 mV V_h. **B** Non-L-, non-N-type channel activity at 0 mV is reduced when V_h is lowered from −90 mV (**B_1**) to −50 mV (**B_2**). Recordings were obtained from an outside-out patch of a chronically ω-CTx-GVIA-treated RINm5F cell containing more than one channel

very short (< 1 min) compared to the average channel run down and (2) the disappearance of channel activity was total and abrupt after toxin application. Usually, channel run down developed gradually in patches containing more than one channel (either L- or non-L-type). The number of active channels decreased progressively trace after trace until they finally disappeared and traces with no channel activity were often followed by traces with some activity. This gradual disappearance was never observed when ω-CTx-GVIA was applied to outside-out patches containing single or multiple HVA channels.

Activity of single Q-like channels resistant to nifedipine and ω-CTx-GVIA could be recorded in excised patches either after acute (Fig. 7A) or chronic application of the toxin (Figs. 7B, 8). In both cases the corresponding non-L-, non-N-type channels exhibited unitary properties very similar to those observed in cell-attached patches. The channel activated at potentials positive to −10 mV (Fig. 8A). The p_o value increased steeply with voltage and reached maximal values above + 30 mV (not shown), with a mean slope conductance of 20.3 pS between −20 and + 20 mV (Fig. 8B). The time course of channel activation was fast at 0 mV and inactivation of ensemble currents was slow and largely incomplete during pulses of 300 ms duration (Fig. 8C). In patches containing multiple channels, channel activity decreased but did not disappear when lowering the holding potential from −90 to −50 mV (Fig. 7B). Channel openings were abolished only at more positive holding potentials (−40 mV, not shown).

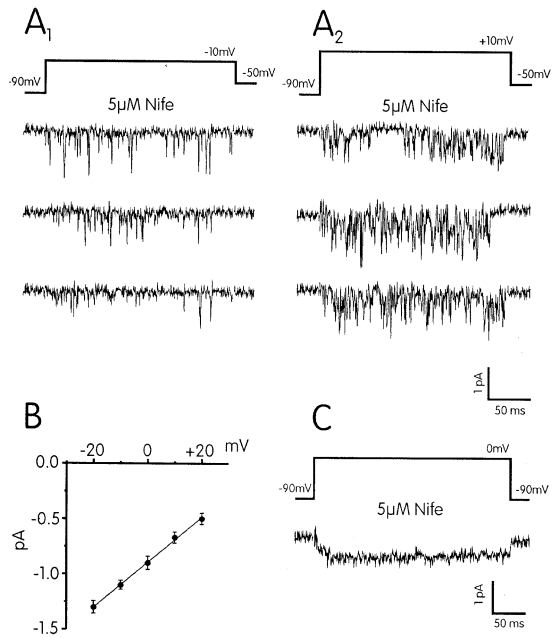

Fig. 8A-C Voltage-dependency and unitary conductance of non-L, non-N-type channels in outside-out patches. **A** Representative recordings of DHP- and ω-CTx-GVIA-resistant channels in an outside-out patch of a ω-CTx-GVIA-treated cell at -10 mV (**A_1**) and + 10 mV (**A_2**). Channel activity was low at -10 mV and increased steeply at + 10 mV. **B** Unitary i/V relationship of the non-L-, non-N-type channel. The regression line through data points has a slope conductance γ, of 20.3 ± 1.2 pS. **C** Ensemble non-N-, non-L-type current obtained by averaging 20 traces recorded under the same conditions as described in **A**. Notice the slow and incomplete inactivation time course of the current

Discussion

Our study provides evidence for the existence of a non-L-, non-N-type channel in RINm5F cells and gives a quantitative description of its elementary properties. The channel is best characterized by its resistance to DHPs and ω-CTx-GVIA and is shown to coexist with the more common L-type channel observed in various β-cells and β-cell lines [27, 28, 35]. Few outside-out patch recordings also provide evidence for a ω-CTx-GVIA-sensitive Ca^{2+} channel with single-channel properties close to the N-type channel described in peripheral neurons [8, 24]. The non-L-, non-N-type channel described here has a high probability of being recorded in patches of ω-CTx-GVIA-treated cells bathed in nifedipine and, therefore, is associated with the Q-like current that contributes to most of the residual non-L, non-N-type current in RINm5F cells [18]. Despite its distinctive pharmacology, the Q-like channel exhibits only subtle differences in the kinetics and permeability properties of the N-type channel of peripheral neurons [24], but deviates partially from the P-type channel of Purkinje neurons [34] and most significantly from the L-type channel of pancreatic β-cells [32].

The L-type channel dominates in insulin-secreting cells and is easily detected in membrane patches of RINm5F cells [35]. Its ubiquity in most patches, however, represents the most serious limitation for the analysis of single non-L-, non-N-type channels and demands suitable conditions for blocking its activity. Our data show unequivocally that addition of 5 μM nifedipine to the external bath, in cell-attached and outside-out patches, is sufficient to abolish single L-type channel activity in 100 mM $[Ba^{2+}]_o$. Nifedipine action is complete, reversible and accompanied by agonistic effects of Bay K 8644 (Fig. 2). In contrast, the insensitivity of channel activity to nifedipine is paralleled by no effects of Bay K 8644 and the corresponding channels are identified as being non-L-type (Fig. 3). Following these criteria, the 24 pS DHP-sensitive channel in RINm5F cells exhibits a kinetics and a single-channel conductance comparable to those of other L-type channels [27, 28, 32]. In agreement with whole-cell current measurements [5, 14], we found that L-type channels activate at more negative potentials if compared to non-L-type HVA channels (Figs. 2 and 5). Single L-type channels are already active around -20 mV and persist at a holding potential of -40 mV. With Bay K 8644, their activation is shifted to even more negative voltages and activities of single Bay K 8644-modified channels are revealed already at -30 and -40 mV (Fig. 1C). There is a significant correlation between the voltage dependence of p_o and the voltage dependency of Ca^{2+} channel conductance derived from whole-cell recordings in 100 mM Ba^{2+} (Figs. 2 and 5). This strengthens the view that pharmacological separation of macroscopic and unitary currents has a high degree of correspondence (see also [32]).

Two non-L-type channels in RINm5F cells.

As expected from previous whole-cell recordings [18, 25], RINm5F cells express two pharmacologically distinct DHP-resistant channels: one sensitive to ω-CTx-GVIA (N-type) and one insensitive to the toxin (non-L-, non-N-type, namely Q-like). Evidence for the existence of two non-L-type channels is mainly based on the irreversible block of Ca^{2+} channels by ω-CTx-GVIA in isolated patches. The ω-CTx-GVIA-sensitive (N-type) and the ω-CTx-GVIA-insensitive (Q-like) channels exhibited otherwise similar biophysical properties. Single-channel conductance (19 vs 21 pS), fast flickering kinetics (τ_o 1.1 vs 0.9 ms at + 10 mV), threshold of activation (> -10 mV), inactivation time course ($\tau_{inact} > 200$ ms) and the sensitivity to holding potential (< -80 mV) were not significantly different. Although we cannot exclude that the ω-CTx-GVIA effect was due to a fast run down of Q-like channels during toxin application, three main pieces of evidence support a genuine block of N-type channels by

ω-CTx-GVIA. First, exposure of active Ca^{2+} channels to the toxin was much shorter (1 min) than the average channel run down (5–10 min). Secondly, the disappearance of channel activity was drastic after toxin application, while channel run down usually developed gradually in patches containing more than one channel. Thirdly, the low probability of finding N-type channels in outside-out patches (3 out of 11) paralleled nicely the proportion of N-type and Q-like currents recorded in RINm5F cells (10–15% vs 30–40%). Apart from this, the N-type channel of RINm5F cells displays close similarities to the N-type channel of other cells. In peripheral neurons the channel activates above -10 mV in 100 mM $[Ba^{2+}]_o$, exhibits a 20 pS single-channel conductance (1.3 pA at + 10 mV), inactivates weakly during prolonged depolarizations and possesses marked sensitivity to holding potential [24]. Indeed, the neuronal N-type channel also exhibits multiple gating modes with low and high p_o [8], small and large conductance and slow and fast inactivation [23] that make any further comparison more complicated and arbitrary.

At variance with the N-type channel, the Q-like channel was easily recorded in both cell-attached and outside-out patches. We found a substantial similarity between cell-attached and outside-out patch recordings of this channel, provided that the patches were treated with ω-CTx-GVIA and bathed in nifedipine-containing solutions. This validates the pharmacological conditions used to abolish N- and L-type channels in cell-attached patches, from which most of the data are derived. The two set of measurements (cell-attached and outside-out) indeed agree in many aspects and suggest distinct properties from those of the L-type channel. The Q-like channel activates at potentials positive to -10 mV and reaches maximal p_o at + 40 mV (Fig. 6B). The L-type channel activates above -20 mV and reaches maximal p_o above + 20 mV. The activity of the Q-like channel is strongly depressed at low holding potentials (≈ -50 mV) while the L-type persists at these values [28]. The channel inactivates little and very slowly irrespective of whether it is recorded in the cell-attached or outside-out configuration, suggesting a marked insensitivity to intracellular Ca^{2+} buffers and a marginal role of Ca^{2+} in the regulation of the channel inactivation gate [20, 25]. In contrast, L-type channels of insulin-secreting cells exhibit marked Ca^{2+}-dependent inactivation properties [20, 22, 25].

The above features exclude the possibility that the non-L-, non-N-type channel may be confused with either the transient LVA T-type channel [4] or with the 19 pS (0.6 pA at 0 mV) low-threshold Ca^{2+} channel described in bullfrog sympathetic neurons [9]. Both channels are insensitive to DHP and ω-CTx-GVIA and are effectively recruited by negative holding potentials; nevertheless they activate at more negative membrane potentials (-30 to -10 mV in 100 mM Ba^{2+}) and inactivate faster than the Q-like channel. They also contribute marginally, if at all, to the total whole-cell current in 100 mM Ba^{2+} (Fig. 1).

The single non-L-, non-N-type channel: Q-like versus P-type

Of the three non-L-, non-N-type channels described in central neurons (Q, P and R; [12, 21, 26]) the one observed in RINm5F cells seems more closely related to the Q-type. The R-type channel described in rat cerebellar granules has kinetic properties sharply different from those illustrated here. It activates at very negative potentials (-40 mV in 10 mM Ba^{2+}) and inactivates quickly and completely within 100 ms [36]. Also the P-type channel is unlikely to correspond to the non-L-, non-N-type observed in RINm5F cells. P-Type channels in cerebellar Purkinje neurons are reported to activate at relatively low membrane potentials (-30 to -20 mV in 10 mM Ba^{2+}; [21]) and to exhibit negligible steady-state inactivation at holding potentials of -40 to -60 mV [34], whereas the non-L-, non-N-type channel in RINm5F cells activates positive to 0 mV and is significantly inactivated at a holding potential of -50 mV [18]. Single P-type channels are also reported to be inhibited by Ca^{2+} channel agonists [34]. We find, in contrast, no inhibitory effects of Bay K 8644 on non-L-, non-N-type channel activity in cell-attached and outside-out patches. A significant presence of P-type channels in RINm5F cells is excluded also by the anomalous blocking effects of ω-Aga-IVA on macroscopic HVA currents. Unlike the P-type current, the non-L, non-N-type current is blocked only at high doses of the toxin (250 nM). In addition, the block by ω-Aga-IVA is reversible and insensitive to repeated membrane depolarizations [18].

A non-L-type channel with kinetics and voltage dependency similar to those of the Q-like channel described here has been reported also in HIT cells [19]. The channel activates positive to 0 mV, is steadily inactivated at low holding potentials and exhibits a persistent fast flickering behaviour. Given the absence of N-type channels in HIT cells [20], the channel is likely to share the same pharmacology of the non-L-, non-N-type channel described here. The two channels may be responsible for the sustained Ca^{2+} current that inactivates in a voltage-dependent manner and is postulated to contribute to the burst duration of β-cell electrical activity [13, 29, 30]. Three Ca^{2+} channel subtypes insensitive to DHP and ω-CTx-GVIA have been reported also in rat cerebellar granule cells (G1, G2, G3; [10]). Among them, the G1-type appears the most closely related to the non-L-, non-N-type of RINm5F cells. The channel has half-maximal probability of activation at + 10 mV, a conductance of 21 pS and sustained bursting activity throughout pulses of 800 ms duration. The channel inactivates steadily at -40 mV

holding potential, is blocked by micromolar applications of ω-CTx-MVIIC (D. Pietrobon, personal communication) and is likely to be associated with a large fraction of the slowly inactivating Ba^{2+} current in granule cells that is insensitive to DHPs and ω-CTx-GVIA [10]. Thus, there seems to be strong biophysical and pharmacological similarity between the non-L-, non-N type channel of RINm5F cells and the G1-type channel of granule cells.

Additional evidence for the existence of a Q-like channel in RINm5F cells comes from the identification in these and other β-cells of a transcript coding for the α_1 subunit of the class A rat brain Ca^{2+} channel [15]. For their pharmacology, α_{1A} subunit channels are commonly associated with Q- rather than P-type channels [26, 36]. Interestingly, a slowly inactivating isoform of the rat brain α_{1A} subunit (rbA-II) with a relatively high-threshold of activation has been reported recently [33]. This strengthens possible homologies between the slowly inactivating Q-like channel and the transcript for the α_{1A} channel subunit in RINm5F cells.

As for other secretory cells in which non-L-, non-N-type channels are shown to control hormone secretion [1, 6, 16], the expression of Q-like channels in insulin-secreting cell lines and the identification of α_{1A} subunits in pancreatic β-cells [15] open the possibility that these channels may be expressed and play a functional role in the control of β-cell electrical activity and hormone release.

Acknowledgements We are grateful to Drs. V. Carabelli, J. Richmond, E. Sher and A. Pollo for a critical reading of the manuscript and to Drs. C. Marchetti and D. Pietrobon for helpful discussions. The financial support of Telethon-Italy (Grant 627 to E.C.) is gratefully acknowledged.

References

1. Artalejo CM, Adams ME, Fox AP (1994) Three types of Ca^{2+} channel trigger secretion with different efficacy in chromaffin cells. Nature 367:72–76
2. Ashcroft FM, Rorsman P (1989) Electrophysiology of the pancreatic β-cell. Prog Biophys Mol Biol 54:201–204
3. Aschroft FM, Kelly RP, Smith PA (1990) Two types of Ca channel in rat pancreatic β-cells. Pflügers Arch 415:504–506
4. Carbone E, Lux HD (1987). Single low-voltage-activated calcium channels in chick and rat sensory neurons. J Physiol (Lond) 386:571–601
5. Carbone E, Sher E, Clementi F (1990) Ca currents in human neuroblastoma IMR32 cells: kinetics, permeability and pharmacology. Pflügers Arch 416:170–179
6. Codignola A, Tarroni P, Clementi F, Pollo A, Lovallo M, Carbone E, Sher E (1993) Calcium channel subtypes controlling serotonin release from human small cell lung carcinoma cell lines. J Biol Chem 268:26240–26247
7. Colquhoun D, Sigworth FJ (1983) Fitting and statistical analysis of single-channel records. In: Sakmann B, Neher E (eds) Single-channel recording. Plenum, New-York, pp 191–263
8. Delcour AH, Tsien RW (1993) Multiple gating modes of N-type Ca^{2+} channel activity distinguished by differences in gating kinetics. J Neuroscie 13:181–194
9. Elmslie KS, Kammermeier PJ, Jones SW (1994) Reevaluation of Ca^{2+} channel types and their modulation in bullfrog sympathetic neurons. Neuron 13:217–228
10. Forti L, Tottene A, Moretti A, Pietrobon D (1994) Three types of voltage-dependent calcium channels in rat cerebellar neurons. J Neuroscie 14:5243–5256
11. Hamill OP, Marty A, Neher E, Sakmann B, Sigworth FJ (1981) Improved patch-clamp techniques for high-resolution current recording from cells and cell-free membrane patches. Pflügers Arch 391:85–100
12. Hillyard DR, Monje VD, Mintz IM, Bean BP, Nadasdi L, Ramachandran J, Miljanich G, Azimi-Zoonooz A, McIntosh JM, Cruz LJ, Imperial JS, Oliveira BM (1992) A new conus peptide ligand for mammalian presynaptic Ca^{2+} channels. Neuron 9:69–77
13. Hopkins WF, Satin LS, Cook DL (1991) Inactivation kinetics and pharmacology distinguish two calcium currents in mouse pancreatic β-cells. Journal of Membrane Biology 119: 229–239
14. Kasai H, Neher E (1992) Dihydropyridine-sensitive and ω-conotoxin-sensitive calcium channels in a mammalian neuroblastoma-glioma cell line. J Physiol (Lond) 448:161–168
15. Ligon BB, Boyd AE (1994) Localization of class A voltage-gated calcium channels in the rat islet. Soc Neuroscie Abstr 20:69
16. López MG, Villaroya M, Lara B, Martinez-Sierra R, Albillos A, García AG, Gandia L (1994) Q- and L-type Ca^{2+} channels dominate the control of secretion in bovine chromaffin cells. FEBS Lett 349:331–334
17. Magnelli V, Pollo A, Lovallo M, Carbone E (1994) DHP-insensitive calcium channels in insulin secreting cells Biophys J 65:A54
18. Magnelli V, Pollo A, Sher E, Carbone E (1995) Block of non-L, non-N-type Ca^{2+} channels in rat insulinoma RINm5F cells by ω-agatoxin IVA and ω-conotoxin MVIIC. Pflügers Arch 429:762–771
19. Marchetti C (1993) Voltage-dependent calcium channels in insulin-secreting cells. Phys Med IX:9–11
20. Marchetti C, Amico C, Podestà D, Robello M, (1994) Inactivation of voltage-dependent calcium current in an insulinoma cell line. Eur Biophys J 23:52–58
21. Mintz IM, Venema VJ, Swiderek KM, Lee TD, Bean BP, Adams ME (1992) P-type calcium channels blocked by the spider toxin ω-Aga-IVA. Nature 355:827–829
22. Plant TD (1988) Properties and calcium-dependent inactivation of calcium currents in cultured mouse pancreatic β-cells. J Physiol 404:731–747
23. Plummer MR, Hess P (1991) Reversible uncoupling of inactivation in N-type calcium channels. Nature 351:657–659
24. Plummer MR, Logothetis DE, Hess P (1989) Elementary properties and pharmacological sensitivities of calcium channels in mammalian peripheral neurons. Neuron 2:1453–1463
25. Pollo A , Lovallo M, Biancardi E, Sher E, Socci C, Carbone E (1993) Sensitivity to dihydropyridines, ω-conotoxin and noradrenaline reveals multiple high-voltage activated Ca^{2+} channels in rat insulinoma and human pancreatic β-cells. Pflügers Arch 423:462–471
26. Randall AD, Tsien RW (1993) Pharmacological dissection of multiple types of Ca^{2+} channel currents in rat cerebellar granule neurons. J Neuroscie 15:2995–3012
27. Rorsman P, Ashcroft FM, Trube G (1988) Single Ca channel currents in mouse pancreatic β-cells. Pflügers Arch 412: 597–603
28. Sala F, Matteson DR (1990) Single-channel recordings of two types of calcium channels in rat pancreatic β-cells. Biophys J 58:567–571
29. Satin LS, Cook DL (1988) Evidence for two calcium currents in insulin-secreting cells. Pflügers Arch 411:1–10
30. Satin LS, Smolen PD (1994) Electrical bursting in β-cells of the pancreatic islets of Langerhans. Endocrine 2:677–687

31. Sher E, Biancardi E, Pollo A, Carbone E, Li G, Wollheim CB, Clementi F (1992) ω-Conotoxin-sensitive, voltage-operated Ca^{2+} channels in rat insulin-secreting cells. Eur J Pharmacol 216:407–414
32. Smith PA, Ashcroft FM, Fewtrell CMS (1993) Permeation and gating properties of the L-type calcium channel in mouse pancreatic β cells. J Gen Physiol 101:767–797
33. Soong TW, Bourinet E, Slaymaker S, Matthews E, Dubel SJ, Vincent SR, Snutch TP (1994) Alternative splicing generates rat brain α_{1A} calcium channel isoforms with distinct electrophysiological properties. Soc Neuroscie Abstr:20:70
34. Usowicz MM, Sugimori M, Cherksey B, Llinas R (1992) P-type calcium channels in the somata and dendrites of adult cerebellar Purkinje cells. Neuron 9:1185–1199
35. Velasco JM (1987) Calcium channels in insulin-secreting RINm5F cell line. J Physiol (Lond) 398:15P
36. Zhang J-F, Randall AD, Ellinor PT, Horne WA, Sather WA, Tanabe T, Schwarz TL, Tsien RW (1993) Distinctive pharmacology and kinetics of cloned neuronal Ca^{2+} channels and their possible counterparts in mammalian CNS neurons. Neuropharmacology 32:1075–1088